Pollution, 5(3): 473-486, Summer 2019
DOI: 10.22059/poll.2018.262231.479
Print ISSN: 2383-451X Online ISSN: 2383-4501
Web Page: https://jpoll.ut.ac.ir, Email: jpoll@ut.ac.ir

Application of Hybrid Cells in Series Model in the Pollution Transport through Layered Material

Chabokpour J.

Civil Engineering Department, Faculty of Engineering, University of Maragheh, Maragheh, Iran

Received: 17.07.2018 Accepted: 22.02.2019

ABSTRACT: The present paper aims at investigating the applicability of hybrid cells in the series model for pollution transport inside the layered porous media. For this purpose, four layers of rock material have fallen inside the experimental flume, with eight sensors installed longitudinally inside the media to obtain experimental BTCs. In order to measure time parameters of the model, named $\boldsymbol{\lambda, T_1, \text{and } T_2}$, two different methods of LSCF and MM have been examined. The model's sensitivity as well as its temporal equations with different parameters have been assessed. Finally, results show that at the fixed time step, the model is more sensitive to $\boldsymbol{\lambda}$ parameter (advection zone time parameter) rather than residential time parameters, to which the moment relations are more sensitive. A detailed computation of the related transport parameters has been operated and the Peclet number, crossing velocity, dispersion coefficient, time to the max, and maximum concentration have been calculated. Eventually, the model's applicability for large-scale porous media has been proven with only one unit of the cells.

Keywords: Layered gravel, HCIS model, plug flow, mixed reservoirs, Peclet number.

INTRODUCTION

Dwindling the water quality affects water supply projects for human use as well as aquatic creatures' life. Therefore, the modeling of the pollution transport is one of the most important issues for engineering of water resources (Chapra 2008; Sharma & Kansal, 2013; Wang et al., 2013; Parsaie & Haghiabi, 2015). Extensive researches, based on pollution transport in different hydraulic media, have been operated by previous investigators, whose main objectives mostly concerned computing the concentration profile efficiently. Nonetheless, every model is constrained by parameter estimation, the accuracy of which totally depends on the precision of estimated parameters, themselves (Chabokpour et al., 2018). Primarily, previous studies have been categorized in three different groups: (I) researches, based on advection-dispersion model, (II) researches, based on estimation of the longitudinal diffusion coefficient, and (III) researches, based on mixing cells (Gosh, 2001). The classical Advection-Dispersion Equation (ADE) is one of the most common models, to be used widely (Chabokpour et al., 2017). Furthermore, there are so many substitute models, presented, instead of undergoing the limitations. The transient storage model (TS) is one, presented due to some problems in the longer tail of extracted breakthrough curves from a river system with dead zone areas (Thackston & Schnelle, 1970; Bencala & Walters, 1983; Beven & Binley, 1992; Harvey & Bencala, 1993;

* Corresponding Author, Email: j.chabokpour@maragheh.ac.ir

Ruddy & Britton, 1989; Runkel, 1998; Fernald et al., 2001; Laenen & Bencala, 2001; Wagener et al., 2002; Schmid, 2003; Wondzell, 2006; Lautz & Siegel 2007; Camacho & Gonzalez-Pinzon, 2008; Tong et al., 2015). The cells in series model (CIS) is another alternative, investigated precisely in the past (Bear, 1972; Banks, 1974; Van der Molen, 1979; Beltaos, 1980; Stefan & Demetracopoulos, l98l; Yurtsever, 1983; Beven & Young, 1988; Young & Wallis, 1993; Wang & Chen 1996). Application of CIS model is limited, due to its inefficiency of advection component (Beer & Young 1984; Rutherford 1994; Ghosh et al., 2008). The hybrid cells in series model was first presented by Gosh (2001) to simulate the breakthrough curves with skewness and also to overcome disadvantages of CIS model. Kumarasamy (2015) operated HCIS within the reaches of Brahmani River by considering first-order decay and reaeration during advection and dispersion process for analysis of temporal and spatial variations of DO parameter. He concluded that in the selected river reaches with special geometric and hydraulic conditions the release of 1180 CMS was required to solve the pollution problems. Kayode & Kumarasamy (2017) focused on the effects of high quantities of nutrients such as ammonia on reduction of DC and consequently, algal propagation in Umgeni River. They offered an analytical solution, based on ammonia propagation through the plug and completely mixed flow zones of HCIS model. In their new developed model, the ammonia kinetic equation was coupled with HCIS model equations, with the concentration variation visualized in different parts of the river. Majority of previous researches concentrated on pollution transport in the river system with some storage area; however, the present study tries to focus on the applicability of HCIS model in the layered rockfill material, operating in many types of hydraulic structures.

MATERIALS AND METHODS

In this model, the total length of any type of hydraulic media got separated into the number of connected units, with each unit consisted of three different reservoirs. The first reservoir was a plug flow zone at the first stage of pollution propagation, the volume, advection time, and initial condition of which was indicated with V_0, λ, and C_i, respectively. The second and third reservoirs were assumed to be thoroughly mixed. The exit concentration from the first reservoir was linked to the second one, and the exit concentration of the second thoroughly mixed reservoir could be regarded as the discharge concentration of the first unit (Gosh, 2001).

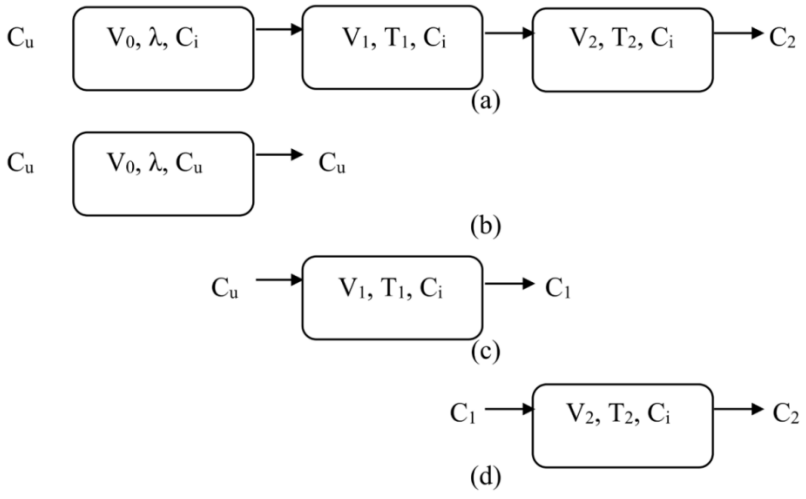

Fig. 1. The conceptual depiction of the transport process in different parts of the model

The equations of the HCIS model were derived by applying the mass balance of the first to third reservoirs (Fig. 1), and outlined as Equations (1) to (16) by the Gosh (2001) and Gosh et al. (2004).

The transport of the model at the plug flow zone can be calculated via Eq. 1 as bellow:

$$C(\lambda u,t)=C_u Dirac(t-\lambda)+\left(1-Dirac(t-\lambda)\right)C_u] \quad (1)$$

where, u represents the average flow velocity and $Dirac$ delta for positive or zero magnitudes is equal to 1 and for negative magnitudes, equal to zero.

By applying the mass balance to the second thoroughly mixed zone, the differential equation can be achieved as Eq. 2:

$$\frac{dC_1(t)}{dt}+\frac{C_1(t)}{T_1}=\frac{C_u Dirac(t-\lambda)}{T_1} \quad (2)$$

Assuming that $t>\lambda$ and also by applying the initial condition of (3), the exact solution of Eq.3 can be computed as Eq. 4.

$$C_1(\lambda)=C_i \ , \ C_2(\lambda)=C_i \quad (3)$$

$$C_1(t)=C_u Dirac(t-\lambda)+(C_i-C_u)e^{-\frac{t-\lambda}{T_1}} \quad (4)$$

The mass balance in the second completely mixed zone results in the differential equation as Eq. 5.

$$\frac{dC_2(t)}{dt}+\frac{C_2(t)}{T_2}=\frac{C_u Dirac(t-\lambda)+(C_i-C_u)e^{-\frac{t-\lambda}{T_1}}}{T_2} \quad (5)$$

The exact solution of Eq. 5 can be obtained as Eq. 6:

$$C_2(t)=C_u Dirac(t-\lambda)+\left(C_i-C_u Dirac(t-\lambda)\right)\times\left[\frac{T_1}{T_1-T_2}e^{-\frac{t-\lambda}{T_1}}-\frac{T_2}{T_1-T_2}e^{-\frac{t-\lambda}{T_2}}\right] \quad (6)$$

By considering the initial concentration as equal to the zero ($C_i=0$), the above equation reduces to Eq. 7 as bellow:

$$c_3(t)=C_u Dirac(t-\lambda)-C_u Dirac(t-\lambda)\times\left[\frac{T_1}{(T_1-T_2)}e^{-\frac{t-\lambda}{T_1}}-\frac{T_2}{(T_1-T_2)}e^{-\frac{t-\lambda}{T_2}}\right] \quad (7)$$

Additionally, by assuming $C_u=1$, the response to the unit step perturbation can represented as Eq. 8:

$$L_3(t)=Dirac(t-\lambda)-Dirac(t-\lambda)\left[\frac{T_1}{(T_1-T_2)}e^{-\frac{t-\lambda}{T_1}}-\frac{T_2}{(T_1-T_2)}e^{-\frac{t-\lambda}{T_2}}\right] \quad (8)$$

Differentiating the $c_3(t)$, with respect to the time variable (t), yields the unit impulse response function as Eq. 9:

$$l_3(t)=\frac{C_u Dirac(t-\lambda)}{(T_1-T_2)}\left[e^{-\frac{t-\lambda}{T_1}}-e^{-\frac{t-\lambda}{T_2}}\right] \quad (9)$$

The time for arriving at the peak can be derived by equating the differential form of Eq. 9 to zero. Afterwards, by substituting the obtained time parameter to the response function, the peak concentration can be achieved (as is presented by Eqs. 10 and 11).

$$t_p(t)=\frac{T_1T_2}{(T_1-T_2)}\ln\left(\frac{T_1}{T_2}\right)+\lambda \quad (10)$$

$$l_3(t_p)=\frac{C_u Dirac(t-\lambda)}{(T_1-T_2)}\left(\left(\frac{T_2}{T_1}\right)^{\left(\frac{T_2}{T_1-T_2}\right)}-\left(\frac{T_2}{T_1}\right)^{\left(\frac{T_1}{T_1-T_2}\right)}\right) \quad (11)$$

Using theoretical convolution technique, as described by Eq. 12, the response of the n[th] unit can be computed as Eq. 13 (Gosh et al., 2008).

$$c_3(n\Delta x,t)=\int_0^t c_3\left((n-1)\Delta x,\tau\right)\times c_3(\lambda,\ T_1,T_2,t-\tau)\,d\tau \quad (12)$$

In which, $c_3(\Delta x,\tau)=c_3(\lambda,T_1,T_2,\tau)$ is the output of the first hybrid unit.

$$c_3(n\Delta x,t)=\frac{Dirac(t-n\lambda)}{(T_1-T_2)^n}\left[\sum_{i=1}^{n}(-1)^{i-1}\frac{n!(t-n\lambda)^{n-i}}{(n-i)!(n-i+1)!}\left(\frac{T_1T_2}{T_1-T_2}\right)^{i-1}\times\left\{\exp\left(-\frac{(t-n\lambda)}{T_1}\right)-(-1)^{n-i}\times\exp\left(-\frac{(t-n\lambda)}{T_2}\right)\right\}\right] \quad (13)$$

where $Dirac(t-n\lambda)=1$ for $t \geq n\lambda$ and $Dirac(t-n\lambda)=0$ for $t \leq n\lambda$

Estimation of HCIS model's parameters requires to use the method of the temporal moments. The general equation in this regard is according to Eq. (14)

$$M_m = \frac{\int_0^\infty t^m c(t)\,dt}{\int_0^\infty c(t)\,dt} \tag{14}$$

In which M_m is the normalized temporal moment with order of m and also, with respect to the time origin.

Application of the above mentioned equation on Eq. 9, with orders of 0 to 4, reduces it to Eqs.15-18 (Gosh, 2001).

$$M_0 = 1 \tag{15}$$

$$M_1 = \lambda + T_1 + T_2 \tag{16}$$

$$M_2 = \lambda^2 + 2\lambda(T_1 + T_2) + 2(T_1 - T_2)^2 + 6T_1T_2 \tag{17}$$

$$M_3 = \lambda^3 + 3\lambda^2(T_1 + T_2) + 6\lambda(T_1 - T_2)^2 + 18\lambda T_1T_2 + 6(T_1 + T_2)(T_1^2 + T_2^2) \tag{18}$$

The experimental data series of the present study had been extracted from an experimental box flume with length, width, and elevation of $(1.8 \times 0.2 \times 0.7)m$, respectively. The layered rock materials, with mean diameters of 3.1, 1.8, 1.1, and 0.8 cm, which also included the porosities of 47%, 44%, 42%, and 41%, were placed inside the flume from coarse to fine respectively. A series of (eight) electrical conductivity sensors operated in order to catch the experimental concentration-time profiles, called Breakthrough curves (BTC). The thickness of every layer was 34.38 cm and the EC sensors were placed 0.02, 17.18, 34.37, 51.56, 68.75, 86, 103.1, and 120.3 cm off the media entrance. After collecting the EC data by means of a designed data logger and software system, the calibration relations of the sensors, presented by the apparatus' manufacturer, was employed to extract the experimental BTC curves. The EC sensors were calibrated by covering the special perimeter of their body and tested in the chemistry laboratory by means of Genway accurate digital instrument. The maximum observed error in the EC sensor system of the present study was reported about 5%.

Fig. 2 gives the schematic diagram of the flume along with the location of the EC sensors' positioning. Also, a real photo of the experimental apparatus is depicted in Fig. 3.

The methodology of the present study can be outlined as below:

First of all, as above mentioned, the experimental BTC data series were extracted in different parts of the layered rockfill material. Here, prior to application of the HCIS model to experimental data, the behavior of the model was explained in details, via variation of its parameters. Afterwards, a sensitivity analysis was done from the model along with temporal moment Equations 1 to 3 to achieve more detailed information about the order of the importance of the parameters in the mentioned equations. The experimental temporal moments 1-3 were calculated and the important transport parameters like velocity, dispersion coefficient, and Peclet number got computed, using the experimental moments along the rockfill media, also exhibited from spatial variation of the mentioned parameters.

The next step entailed extracting the HCIS time parameters for a plug flow zone as well as double completely-mixed zones via considering the experimental data series. Afterwards, the theoretical BTCs were constructed and compared with the experimental ones, using statistical parameters.

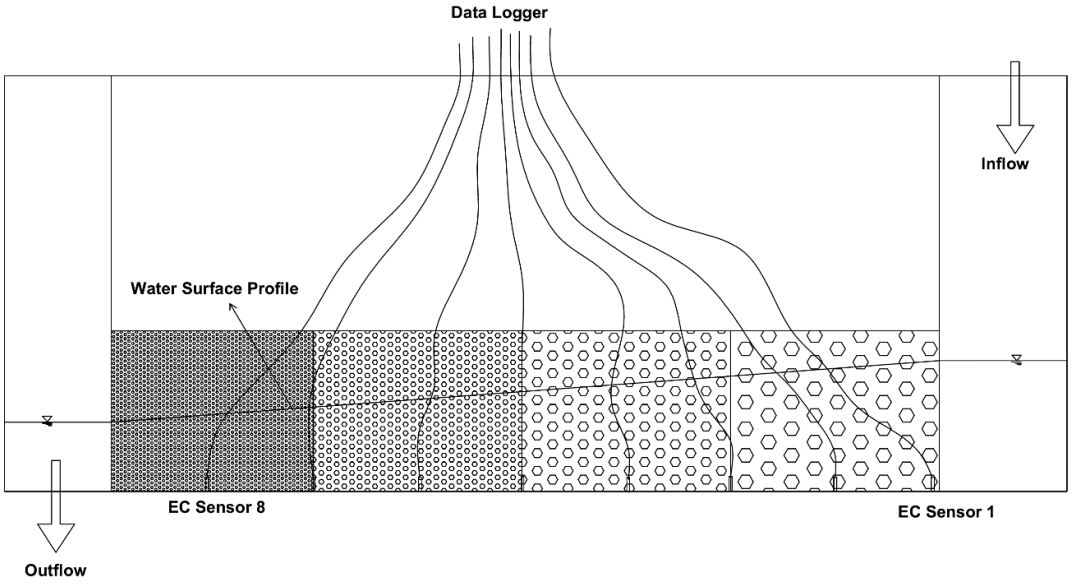

Fig. 2. Schematic layout of the layered material and the sensors' locations

Fig. 3. A real photo from different parts of the experimental apparatus

RESULTS AND DISCUSSION

In the current section, firstly tries to present a short review about the behavior of the model through altering its parameters in accordance with the presentation of the model providers, on one hand (Gosh, 2001; Gosh et al., 2004; Gosh et al., 2008), and mathematical approach of the current paper's author, on the other.

The parameters of this model varied in such a way that different shapes of the BTCs appeared. Fig. 4 demonstrates the results. It can be seen that variation in the residence time for both completely-mixed reservoirs shows the same result in shape of the response function (Eq. 9, where $C_u = 1$). Accordingly, increased residence times leads to a dispersive shape of BTC with longer downward limb and lower peak concentration (Fig. 4 (a and b)). Previous investigators mentioned that the reservoirs' residence time was interchangeable, i.e., even though the reservoirs' size was unequal, it did not matter to which the solute entered firstly. Despite what is said about the residence time of completely-mixed reservoirs, raising the residence time in the plug flow zone of the model did not result in any change in shape of the BTC, and only the transportation of BTC was observed in the time axis. Finally, it is evident that although the value of both T_1, T_2 parameters had the same effect, the λ parameter showed a different effect on the shape of the BTC.

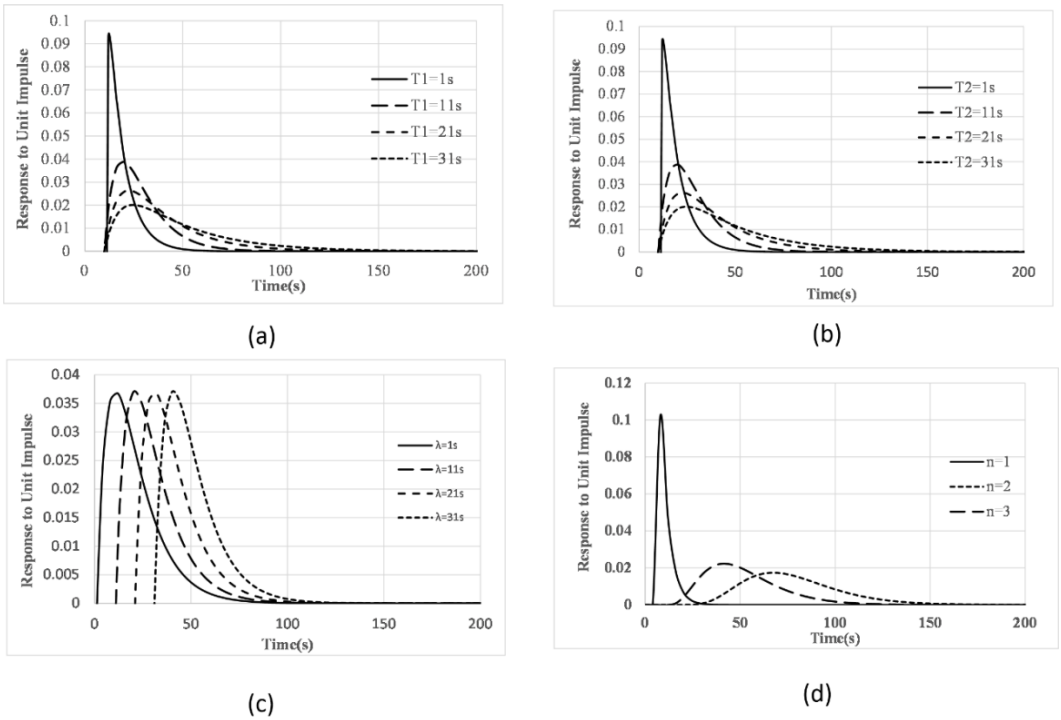

Fig. 4. Variation in the shape of BTC a) λ= 10s, T_1= 8s, T_2= (1 … 31)s, b) λ= 10s, T_1= (1 … 31)s, T_2= 8s c) λ= (1 … 31)s, T_1= 12s, T_2= 8s, and d) variation in the number of units

Another parameter of the model to be examined is the number of the units. According to Eq. 15, it can be concluded that through the rise of the number of the units, the solute is propagated longitudinally, making the BTC more symmetrical, with its shape changing like what is shown in Fig. 4 (d). In the present study, all reaches inside the rockfill media are considered one separate unit.

In order to examine the sensitivity analysis of HCIS model and the related temporal moment equations, with respect to the time origin from 1 to 3, all of the time parameters were normalized according to Eq. 19:

$$x_n = \frac{(x_i - \bar{x})}{std(x_i)} \tag{19}$$

where, x_n is the normalized parameter; x_i, the real parameter; $\bar{x}$, the mean of the real parameter; and $std(x_i)$, the standard deviation of the real parameter.

Once the time parameters got normalized, both effects and intensity of parameters' changes on the model output BTC were studied. As concluded and depicted in Fig. 5 (a), at the fixed time, increase of the λ parameter shows an increasing impact on the concentration, while the rise of the residence time parameters $(T_1 \; and \; T_2)$ indicates a decreasing one. Computation of the changes' slope shows that the slope of the change of concentration around $x_n = -1.5$ was indicative of a very steep decreasing tendency (Fig. 5 (b)). Generally, it can be said that increasing the time of advection, in the fixed time step of the breakthrough curve, implied a steeper enhancing trend rather than the residential dispersion time. Moreover, it seems that the model was more sensitive to the advection time parameter rather than residential time parameters in the thoroughly mixed reservoirs even though their effect was reversed.

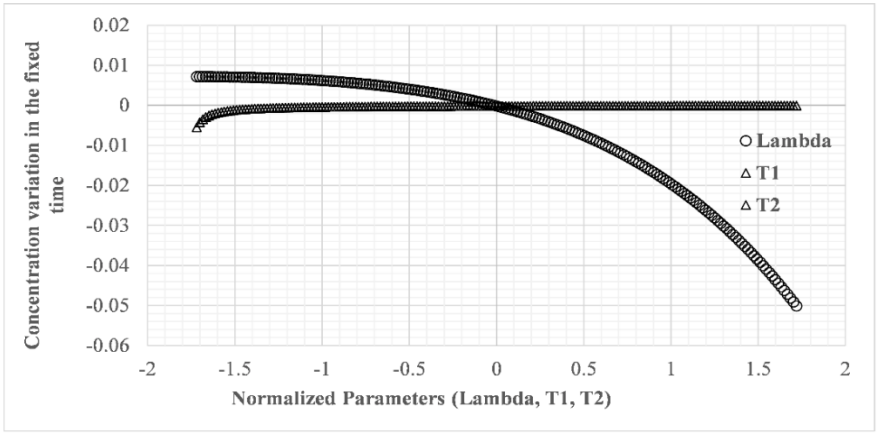

(a)

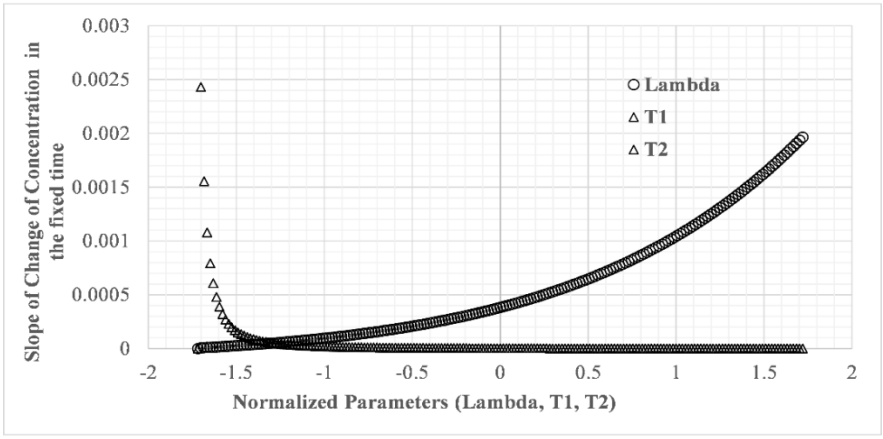

(b)

Fig. 5. a) Concentration variation, b) slope of concentration change versus time parameters of the model

Application of the general relation of the temporal moment (Eq. 12), for the moments from 1st to 3rd, reduced to Eqs. 14-16, respectively. By considering and examining them with normalized parameters, as depicted in Fig. 6, it can be understood that all of the moments would be increased through rising the time parameters, though this sentiment and the slope of changes showed a different set of modulates, e.g., the first moment varied linearly with all of the time parameters, but the other orders stated a non-linear trend. As an addition, it was concluded that the residential time parameters of dispersion reservoirs had a more intense impact on the 2nd and 3rd moment equations. Another important issue, worthy to mention, is that the first to third moments of the breakthrough curves explained the convection time, dispersion characteristics, and skewness of the hydraulic media, respectively; therefore, the orders of the magnitudes of these parameters differed largely from one another. By taking into account the rate of changes, as aforementioned, the first moment did not show any slope commutation via variation of the time parameters, while 2nd moment explained the linear slope with further effects of the residential time parameters and the 3rd one showed the power type slope change. As a general inference, it can be said that with the exception of the first moment equation, the other moment equations were more sensitive to the residential time parameters rather than advection time parameter.

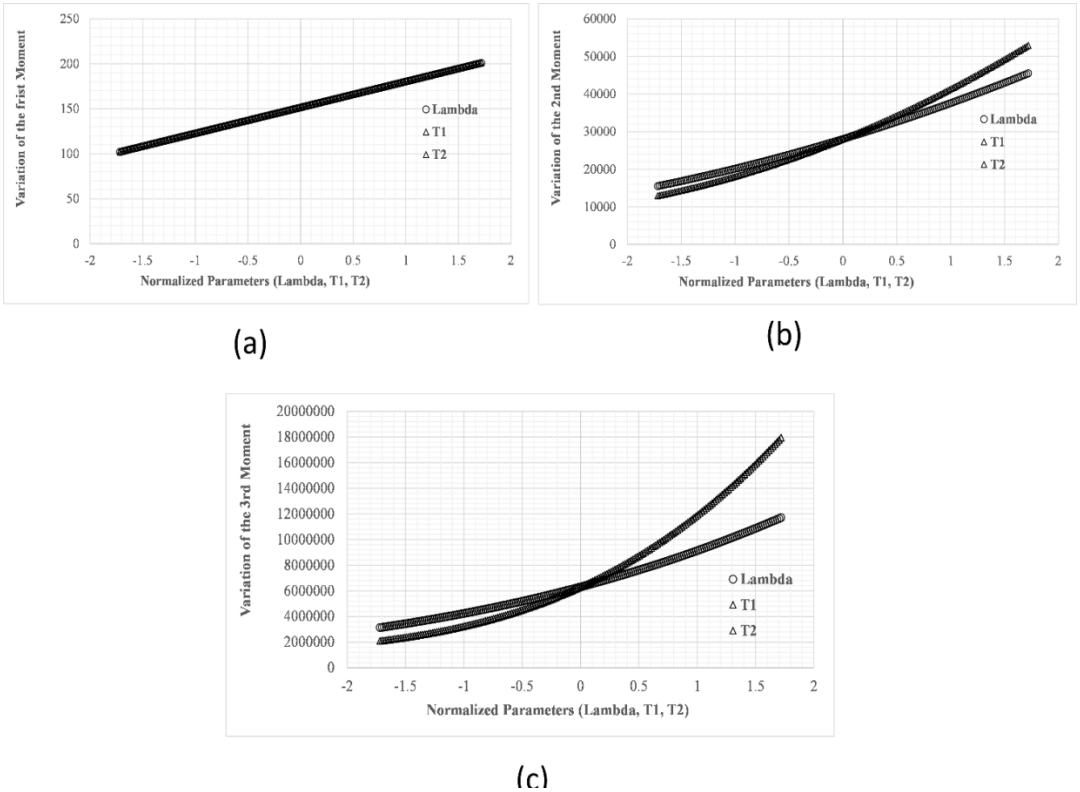

Fig. 6. Variation of the a) first, b) second, and c) third temporal moments versus normalized time parameters of HCIS model

The normalized moments for eight experimental BTC curves, located in different parts of the layered material, were calculated, using Eq. 12, with the results illustrated in Fig. 7. It was derived that the moments from 1st to 4th can be related linearly to the distance parameter, but the R^2 for the first moment surpassed the 4th one, meaning that their linear inclination kept getting weaker as the order of the moments rose. Fig. 7 illustrates all of their regression relations. Other two parameters of the experiments (entrance discharge and entrance concentration) were also tested by the moment equations. As illustrated in different parts of Fig. 7, by enhancing the entrance discharge, the normalized moment values declined, meaning that the solute passed with a higher concentration at the same time, compared with lower entrance discharges. In the normalized moment equation, the numerator was related to time step and concentration, but the denominator was only related to the concentration. The growth of the entrance discharge would cause a reduction of BTC concentration and, consequently, the quantities of the moments. Despite what was observed about entrance discharges, detracting or enhancing the entrance concentration, also completely related to the numerator and denominator of the Eq. 12, did not demonstrate any significant impact on the normalized moments' magnitude. It should also be mentioned that the moments themselves would ascend through enhancement of the entrance concentration, not the normalized ones.

In the present study, according to the relations of the Gosh et al., (2008), obtained through comparison of the HCIS model with a classical ADE equation, the Peclet number, real crossing velocity, and the dispersion coefficients, were calculated corresponding to Eqs. 20-22.

$$u = \frac{\Delta x}{M_1} \tag{20}$$

$$Pe = \frac{2M_1^2}{M_2 - M_1^2} \quad (21)$$

$$D = \frac{\Delta x \times u}{Pe} \quad (22)$$

where u is real crossing velocity; Δx, the unit length; M_1, the normalized first moment; M_2, the normalized second moment; Pe, the Peclet number; and D, the dispersion coefficient.

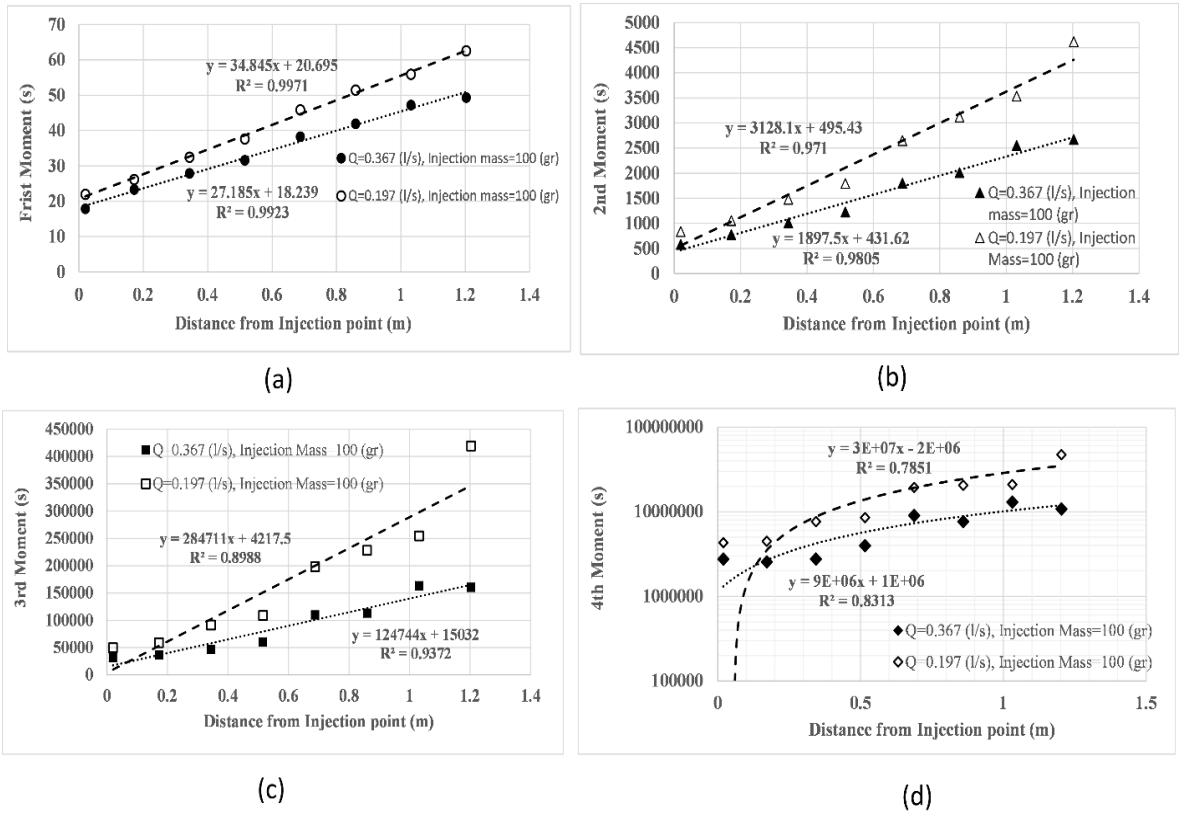

Fig. 7. The real values of the a) first, b) second, c) third, and d) fourth temporal moments versus distance from injection point

With the exception of the first experimental BTC, for other BTCs the values of Pe number stood above 4, which signified that the mean residence time of the HCIS and ADE models were nearly the same. For data series of the present study, the Pe number showed a mounting linear trend with the length parameter of each unit. Fig. 8 gives the regression equations between them. By taking into account the upstream discharge and concentration, it was understood that the Pe number would be affected directly by increasing the entrance discharge, though the upstream concentration did not show any impact on the quantities of the Pe number. Also, same inclination was observed about the real crossing velocity. Since it is related directly to the length of the unit and reversely to the first moments, results show its increase via enhancing the length parameter. Also, as aforementioned, addition of the entrance discharge would directly affect the crossing velocity, while the upstream concentration would not. The classical ADE equation only depended on the one important parameter of the dispersion coefficient. Through the mathematical approach of HCIS model owners, the model parameters, called

λ, T_1 and T_2, were related to the dispersion coefficients and according to Eq. 20, its magnitudes were calculated for all eight experimental BTCs, with the results depicted in the Fig. 8 (e and f), making it possible to conclude that increase of the length parameter would raise the dispersion coefficients and cause symmetrical shape in the BTC. No parameter of entrance discharge and upstream concentration showed any significant effect on the values of the dispersion coefficients.

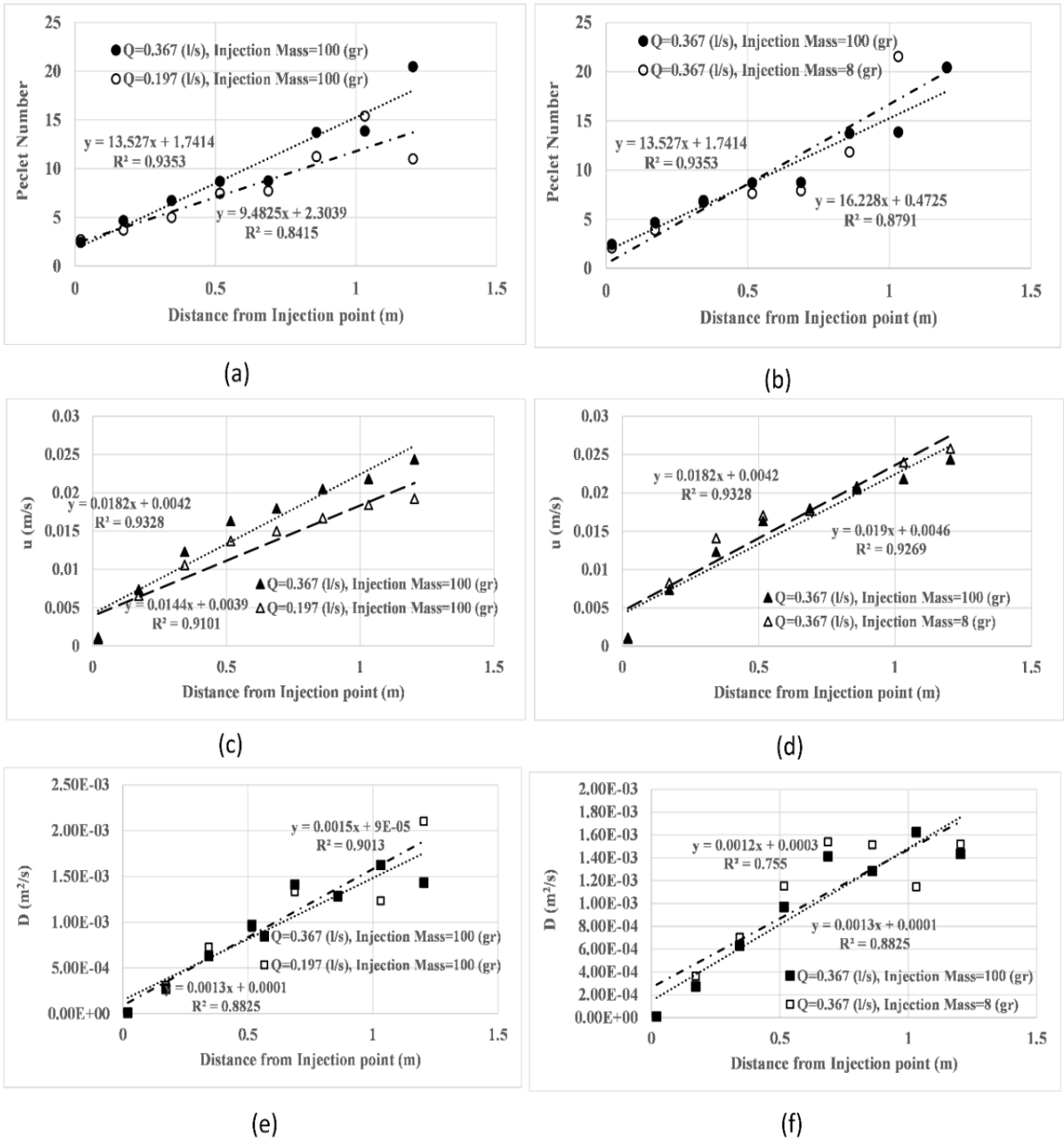

Fig. 8. a) Peclet number for different entrance discharges versus distance parameter, b) Peclet number for different entrance concentrations versus distance parameter, c) real crossing velocity for different entrance discharges versus distance parameter, d) real crossing velocity for different entrance concentrations versus distance parameter, e) dispersion coefficients for different entrance discharges versus distance parameter, f) dispersion coefficients for different entrance concentrations versus distance parameter

The parameters of HCIS model were calculated with two different methods of the least square curve fitting (LSCF) and the simultaneous solution of the three moment equations (MM). The results indicated that, totally, the former method (LSCF) was better for parameter estimation and the recreation of the theoretical breakthrough curves rather than the latter (MM). The λ parameter, which depended on the size of the plug flow zone, indicated the magnitudes' boosting through improvement of the length scale in both methods. The obtained values for λ parameter, from both methods, was close to each other, not being affected by any variation of the entrance discharges and upstream concentrations. The overall size of the completely-mixed zones, capable of being illustrated with $T_1 + T_2$ parameter and related to the volume of the reservoirs, was also examined and the conclusions implied that like λ parameter, LSCF was a better method for estimation of the residence time parameters rather than MM; however, the sum of the estimated time parameters $(\lambda + T_1 + T_2)$ was unnecessarily equal to the first temporal moment. Like other figures, the regression equations have been placed over different parts of Fig. 9.

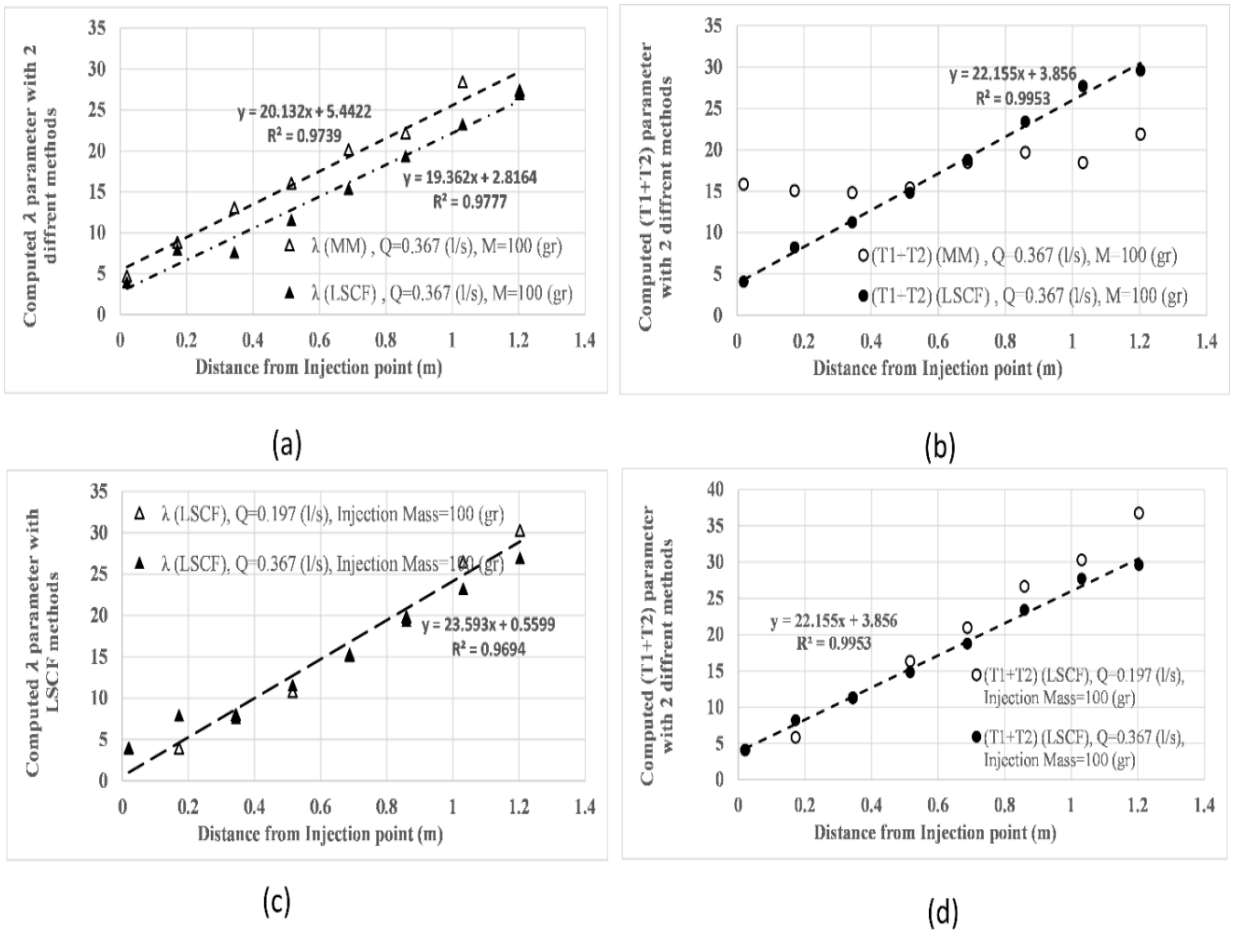

Fig. 9. a) Calculated λ parameter with two different methods of LSCF and MM versus distance parameter, b) calculated $T_1 + T_2$ parameter with two different methods of LSCF and MM versus distance parameter, c) examination of the variation in the entrance concentration with λ parameter, d) examination of the variation in the entrance discharge with $T_1 + T_2$ parameter

Through operation of calculated time parameters of HCIS model, the theoretical concentration curves had been calculated and illustrated against the experimental data series in three different positions of the layered rockfill media (Fig. 10). Results show a good correspondence with the experimental data series and the advection with dispersion processes of the solute transport, being evident in both. The statistical parameters of the root mean square error (RMSE), Nash- Sutcliffe (DC), and mean absolute error (MAE) was calculated to exhibit the goodness of the model's fitting with the experimental data series and consequently the magnitudes of the RMSE=0.068, DC=0.92, and MAE=73 (ppm) were obtained, which confirmed the applicability of the model.

All of the recreated theoretical BTCs were obtained by application of the only one single unit and its related time parameters. Therefore, it can be seen that in such a condition with large porous media, which totally had a smaller length scale rather than natural rivers, application of the only one unit was efficient. Calculated residence time parameters (T_1, T_2) For very small distances, e.g., first three sensors, demonstrated very negligible quantities, implying that in the very low distances application of only one completely-mixed reservoir could be done.

The time for reaching maximum concentration and the maximum concentration are also two important parameters in the solute transport experiments. The mentioned parameters of the present study got computed and depicted in Fig. 11. It is evident that through the descending motion of the solute cloud inside the pore system of the layered material, the time to reach the maximum parameter mounted. Similarly in lower discharges, the same phenomenon occurred, this time because of lower values of the crossing velocity. On the other hand, the downward motion of the cloud led to this reduction, showing higher values in lower discharges of the maximum concentration.

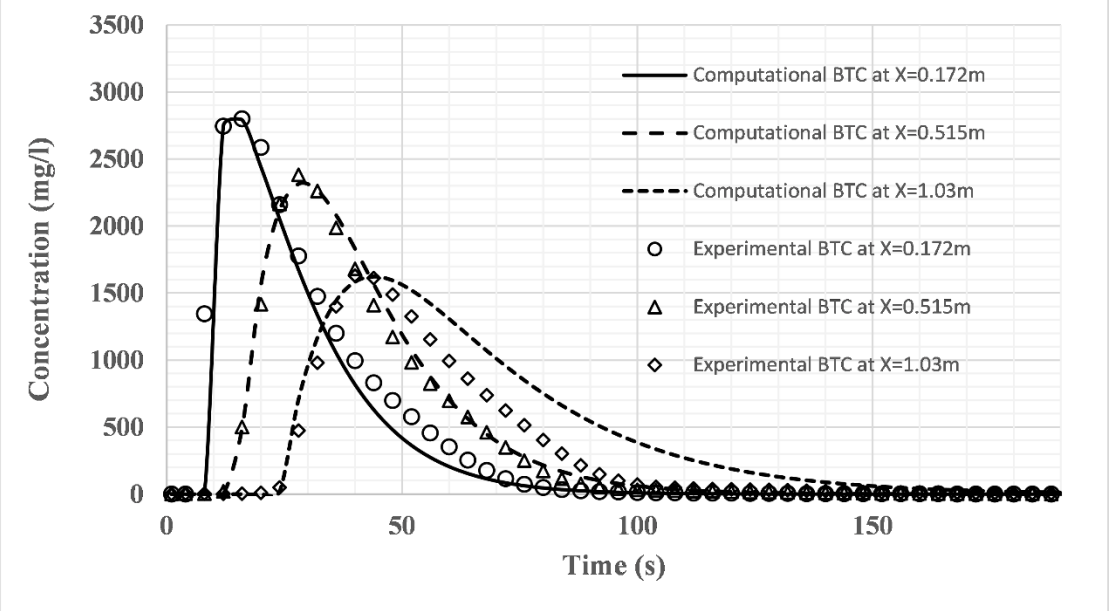

Fig. 10. Experimental and computational breakthrough curves in three different positions of the layered rock fill material for an injection mass of 30gr and entrance discharge of 0.197 (l/s)

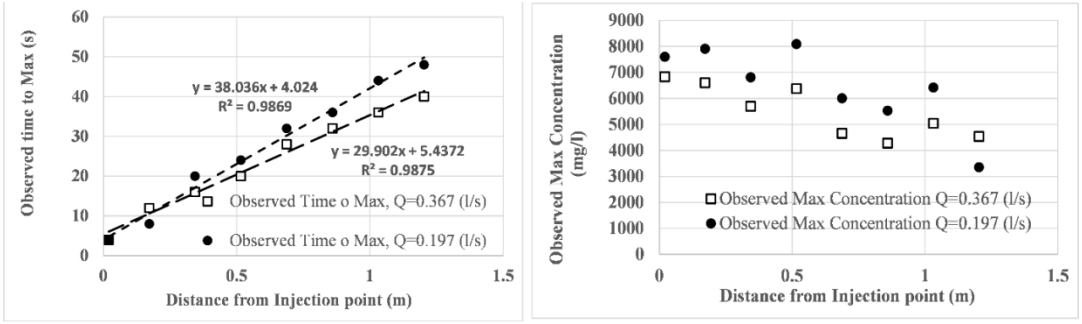

Fig. 11. Observed time of reaching the maximum concentration and maximum concentration, itself, for two different discharges with injection mass equal to 100 (gr)

CONCLUSION

The present study helped proving the applicability of the hybrid cells in series model in the solute transport through large porous medium, by operation of only one unit. Of both LSCF and MM Methods, the former turned out to be a better method for parameter estimation of HCIS method. The model behavior was examined by varying its parameters, leading to different shapes of BTC. The experimental temporal moments were calculated and their increase by distance parameter was concluded. Also, these magnitudes got to be identified as a useful tool to estimate the model's parameters. By employing the correlated parameters of HCIS and ADE classical models, the transport parameters like dispersion coefficients, real crossing velocity, and Peclet number were computed and the transport process was interpreted. Finally, through operation of the extracted parameters, the theoretical breakthrough curves were both calculated and depicted against experimental ones and their comparison confirmed the applicability of HCIS for solute transport through large porous media. The mentioned large porous media generally exists in groundwater around river systems; quality analysis of the spring systems, flowing in rocky media; pollution transport inside the detention rockfill dams; and so many hydraulic structures, constructed from such materials.

REFERENCES

Banks, R. B. (1974). A mixing cell model for longitudinal dispersion in open channels. Water Resour. Res., 10, 357–358.

Bear, J. (1972). Dynamics of fluids in porous media, American Elsevier, New York.

Beltaos, S. (1980). Longitudinal dispersion in rivers. J. Hydr. Div., Am. Soc. Civ. Eng., 106(I), 151–171.

Bencala, K.E. and Walters, R.A. (1983). Simulation of solute transport in a mountain pool and riffle stream-a transient storage model. Water Resour. Res., 19:718–724.

Beven, K. J., and Young, P. C. (1988). An aggregated mixing zone model of solute transport through porous media." J. Contam Hydrol., 3, 129–143.

Beven, K. J. and Binley, A. M. (1992). The future of distributed models: Model calibration and uncertainty prediction. Hydrolo. Pro., 6, 279–298.

Camacho, L. A. and Gonzalez-Pinzon, R. (2008). Calibration and prediction ability analysis of longitudinal solute transport models in mountain streams. J. of Envi. Flu. Mecha., 8(5), 597–604.

Chabokpour, J., Samadi, A. and Merikhi, M. (2018). Application of method of temporal moments to the contaminant exit breakthrough curves from rockfill media. Iran J. Soil Water Res., 49(3):629-640.

Chabokpour, J., Minaei, O. and Daneshfaraz, R. (2017). Study of the Longitudinal Dispersion Coefficient of Nonreactive Solute through the Rockfill Medium. J. of Hydraulic, 12(2): 1-12.

Chapra, S. C. (2008). Surface water quality modelling. Waveland press

Fernald, A.G., Wigington, J.P.J. and Landers, D.H. (2001). Transient storage and hyporheic flow along the Willamette River, Oregon: field measurements and model estimates. Water Resour. Res., 37: 1681–1694.

Ghosh, N. C. (2001). Study of solute transport in a river. Ph.D. thesis, I.I.T, Roorkee, India.

Ghosh, N. C., Mishra, G. C., and Ojha, C. S. P. (2004). A hybrid-cells in-series model for solute transport in a river. J. Environ. Eng., 13010, 1198–1209.

Ghosh, N. C., Mishra, G. C., and Kumarasamy, M. (2008). Hybrid-Cells-in-Series Model for Solute Transport in Streams and Relation of Its Parameters with Bulk Flow Characteristics. J. Hyd. Engng., 134:497-502.

Harvey, J.W. and Bencala, K.E. (1993). The effect of streambed topography on surface–subsurface water exchange in mountain catchments. Water Resour. Res., 29: 89–98.

Kayode, O. O., and Kumarasamy, M. (2017). Development of the hybrid cells in series model to simulate ammonia nutrient pollutant transport along the Umgeni River. Environ. Sci. Pollut. Res., 24:22967–22979.

Kumarasamy, M. (2015). Deoxygenation and reaeration coupled hybrid mixing cells based pollutant transport model to assess water quality status of a river. Int. J. Environ. Res., 9:341–350.

Laenen, A. and Bencala, K.E. (2001). Transient storage assessments of dye-tracer injections in rivers of the Willamette Basin. J. of the American Water Reso. Asso., 37: 367–377.

Lautz, L.K. and Siegel, D.I. (2007). The effect of transient storage on nitrate uptake lengths in streams: an inter-site comparison. Hydro. Proc., 21: 3533–3548.

Parsaie, A., and Haghiabi, A.H. (2015). Computational modelling of pollution transmission in rivers. Appl. Water Sci., Pp.1-10.

Ruddy, B.C. and Britton, L. J. (1989). Travel time and Re aeration of Selected Streams in the North Platte and Yampa River basins, Colorado. U.S. Geological Survey Water Resources Investigations Report, 88–4205;56.

Runkel, R.L. (1998). One Dimensional Transport with Inflow and Storage (OTIS): a Solute Transport Model for Streams and Rivers. Water Resources Investigations Report, US Geologic Survey, 98–4018.

Rutherford, J. C. (1994). River mixing, Wiley, Chichester, England

Schmid, B. H. (2003). Temporal moments routing in streams and rivers with transient storage, Advan. in Water Reso., 26, 1021–1027.

Sharma, D., and Kansal, A. (2013). Assessment of river quality models: a review. Rev. Environ. Sci. Bio., 12:285–311.

Stefan, H. G., and Demetracopoulos, A. C. (1981). Cells in series simulation of riverine transport. J. Hydr. Div., 1076, 675–697.

Tong, Y. and Deng, Z. Q. (2015). Moment-Based Method for Identification of Pollution Source in Rivers, J. of Env. Engng., 141(10), 1-27.

Thackston, E.L. and Schnelle, K.B.J. (1970). Predicting effects of dead zones on stream mixing. J. of the Sanitary Engng. Divi., 96: 319–331.

Van der Molen, W. H. (1979). Salt balance and leaching requirement. Drainage principles and applications. Publication No. 16, Vol. II, Int. Institute for Land Reclamation and Improvement, Wageningen, The Netherlands.

Wagener, T., Camacho, L.A. and Wheater, H.S. (2002). Dynamic identify ability analysis of the transient storage model for solute transport in rivers, J. of Hydro. Infor., 4(3), 199–211.

Wang, Q., Li, S., and Jia, P. et. al. (2013). A review of surface water quality models. Sci. World J. 2013:1–7.

Wondzell, S.M. (2006). Effect of morphology and discharge on hyporheic exchange flows in two small streams in the Cascade Mountains of Oregon, USA. Hydro. Proc., 20: 267–287.

Wang, G. T., and Chen, S. (1996). A new model describing convective dispersive phenomena derived using the mixing-cell concept. Appl. Math. Model, 20, 309–320.

Young, P. C. (1984). Recursive estimation and time series analysis: An introduction, Springer, Berlin.

Young, P. C., and Wallis, S. G. (1993). Solute transport and dispersion in channels. Channel network hydrology, K. Beven and M. Kirkby, eds., Wiley, New York, 129–171.

Yurtsever, Y. (1983). Models for tracer data analysis. Guidebook on nuclear techniques in hydrology, International Atomic Energy Agency, Vienna, Austria, 381–402.

Pollution is licensed under a "Creative Commons Attribution 4.0 International (CC-BY 4.0)"